312 Bull. Chem. Soc. Jpn. Vol. 84, No. 3, 312–319 (2011) © 2011 The Chemical Society of Japan

Odd–Even Effect and Unusual Behavior of Dodecyl-Substituted Analogue Observed in the Crystal Structure of Alkyltrimethylammonium–$[Ni(dmit)_2]^-$ Salts

Kotaro Dai,* Kuniharu Nomoto, Shinji Ueno, Kazuaki Tomono, and Kazuo Miyamura

Department of Chemistry, Faculty of Science, Tokyo University of Science,
1-3 Kagurazaka, Shinjuku-ku, Tokyo 162-8601

Received November 2, 2010; E-mail: j1307706@ed.kagu.tus.ac.jp

A series of $[Ni(dmit)_2]^-$ (dmit: 1,3-dithiole-2-thione-4,5-dithiolato) salts of alkyltrimethylammonium (**C*n***: *n* represents the alkyl chain length; $n = 3$ and 5–18) have been prepared and analyzed by X-ray structural analysis. All complex salts have been found to be composed of alternate sheets of $[Ni(dmit)_2]^-$ anions and sheets of cations with a pronounced interdigitation of the alkyl chains. However, molecular arrangement differed between (**C3**)$[Ni(dmit)_2]$ and other (**C*n***)$[Ni(dmit)_2]$ ($n = 5$–18). Adjacent cations were aligned along the long axis of $[Ni(dmit)_2]^-$ anion in **C3** complex salt, while in others (**C5**–**C18** complex salts), they were aligned toward the short axis. Such a difference in arrangement arose from correlativity between the lengths of the long axis of cation and anion, namely **CLCA**. Furthermore, relative orientation between the alkyl chain of cation and $[Ni(dmit)_2]^-$ anion differed between the odd- and even-numbered cations for **C10**–**C18**. Whereas the plane of alkyl chain for odd-numbered cation was normal to the plane of $[Ni(dmit)_2]^-$ anion, that of even-numbered cation was parallel. It was also found that **C12** analog behaved like odd-numbered cations. However, in **C12** salt, the end methyl group of the dodecyl group adopted unusual end-*gauche* conformation.

Alkyl chains are commonly used to promote the solubility of organic rigid compounds such as, for example, polymers and aromatic compounds, and octyl or dodecyl groups are usually used because of their availability.[1–8] The reason simply arises from the fact that alkyl chains provide good solubility in various kinds of organic solvents due to its hydrophobicity. Therefore, most of these reported results pay less attention to the length of alkyl chains they use. On the other hand, it is well-known that compounds with long alkyl chains exhibit odd–even effect depending on their chain length in various physical properties, such as melting points, heats of fusion, TOF-SIMS spectra and 2D molecular arrangements.[9–16] This effect on the molecular conformation in the crystal structure has also been reported,[17,18] but such structural consideration is quite rare so far.

Meanwhile, over the past two decades, an enormous amount of research has gone into the synthesis and characterization of transition metal–bis(dithiolato) complexes of dmit (dmit: 1,3-dithiole-2-thione-4,5-dithiolato) and its extended π-conjugated derivatives.[19–21] Among the vast number of studies reported so far, a great deal of attention has been focused on the development of electrically conductive Langmuir–Blodgett (LB) membrane systems based on alkylammonium–[metal-$(dmit)_2$] (metal = Ni, Au, Pt, Pd, Zn, and Cu) salts and related compounds.[22,23] In order to understand the correlation between the structure and the electrical properties of thin films thus constructed, analysis of the bulk crystal structure is of particular importance, because it can be used to predict the local stable structure of the thin films. Some studies with single-crystal X-ray analysis are already reported.[24–26] However, systematic studies on the structural change brought about by the change in the alkyl chain length have drawn less attention. Since physical properties including electric conductivity of molecule-based materials depend primarily on the molecular arrangement, systematic and thorough research on the intra- and intermolecular interaction is required to predict the exact structure of the material, especially in the crystalline state, and thus their properties. From this point of view, we have been investigating the structure of $[Ni(dmit)_2]^-$ complex salts of cations with long alkyl chains (Chart 1). We expected a new arrangement of $[Ni(dmit)_2]^-$ anions regulated by intermolecular interaction of long alkyl chains.[27–31] As shown in our previous report, the use of dodecyltrimethylammonium as cation resulted in formation of characteristic cation aggregate by hydrophobic interaction in the crystal. In this work, the structural change in crystals of $[Ni(dmit)_2]$ complex salts

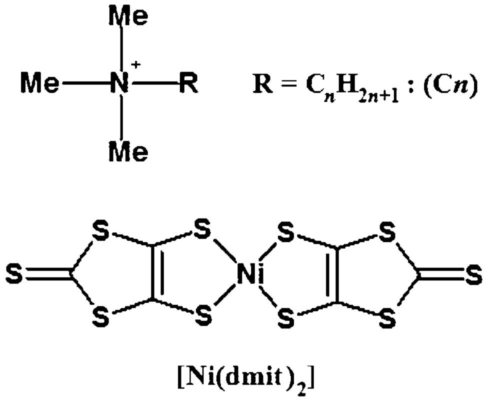

Chart 1.

Published on the web March 4, 2011; doi:10.1246/bcsj.20100306

depending on the alkyl chain length of alkyltrimethylammonium cations is reported.

Experimental

Synthesis of Alkyltrimethylammonium (C*n*) Bromide. Trimethylamine (2.36 g, 10 mmol) and alkyl bromide (12 mmol) were stirred in acetonitrile (25 mL) for 48 h. Acetonitrile was then evaporated to obtain a crude product. A small amount of methanol, diethyl ether, or a mixture of these was added to the residue to give a white powder. This powder was washed with diethyl ether and dried in vacuo over night.

Synthesis of (C*n*)[Ni(dmit)$_2$] Salts. 4,5-Di(thiobenzoyl)-1,3-dithiole-2-thione (dmit(COPH)) was synthesized by a reported method.[32] Obtained dmit(COPh)$_2$ (920 mg, 2.25 mmol) was treated with an excess of sodium methoxide (0.5 M) in methanol (20 mL) under nitrogen at room temperature with stirring. To the resulting dark red solution, $NiCl_2 \cdot 6H_2O$ (238 mg, 1 mmol) in methanol (20 mL) and alkyltrimethylammonium (**C*n***) bromide (2.4 mmol) in methanol (20 mL) were added successively. The resulting precipitate was washed with methanol. All complex salts were obtained by oxidizing this precipitate in acetone using I_2 and NaI according to a literature procedure. The resultant black crystal was collected by filtration, and purified by recrystallization using a mixed solvent of acetone and methanol. Single crystals were grown by slow evaporation from acetone and methanol solution of complex salt at room temperature. Unfortunately, single crystals suitable for X-ray crystal structural analysis were not obtained for (**C2**)[Ni(dmit)$_2$] and (**C4**)[Ni(dmit)$_2$].

(**C3**)[Ni(dmit)$_2$]; Anal. Found: C, 26.23; H, 2.64; N, 2.90%. Calcd for $C_{12}H_{16}NS_{10}Ni$: C, 26.03; H, 2.91; N, 2.53%. IR (KBr): 1345 cm^{-1} for $\nu_{(C=C)}$, 1053 cm^{-1} for $\nu_{(C=S)}$.

(**C5**)[Ni(dmit)$_2$]; Anal. Found: C, 29.22; H, 3.28; N, 2.43%. Calcd for $C_{14}H_{20}NS_{10}Ni$: C, 28.91; H, 3.47; N, 2.41%. IR (KBr): 1349 cm^{-1} for $\nu_{(C=C)}$, 1061 cm^{-1} for $\nu_{(C=S)}$.

(**C6**)[Ni(dmit)$_2$]; Anal. Found: C, 30.25; H, 4.00; N, 2.27%. Calcd for $C_{15}H_{22}NS_{10}Ni$: C, 30.24; H, 3.72; N, 2.35%. IR (KBr): 1350 cm^{-1} for $\nu_{(C=C)}$, 1059 cm^{-1} for $\nu_{(C=S)}$.

(**C7**)[Ni(dmit)$_2$]; Anal. Found: C, 31.88; H, 3.99; N, 2.23%. Calcd for $C_{16}H_{24}NS_{10}Ni$: C, 31.52; H, 3.97; N, 2.30%. IR (KBr): 1351 cm^{-1} for $\nu_{(C=C)}$, 1059 cm^{-1} for $\nu_{(C=S)}$.

(**C8**)[Ni(dmit)$_2$]; Anal. Found: C, 32.91; H, 4.10; N, 2.30%. Calcd for $C_{17}H_{26}NS_{10}Ni$: C, 32.73; H, 4.20; N, 2.25%. IR (KBr): 1351 cm^{-1} for $\nu_{(C=C)}$, 1059 cm^{-1} for $\nu_{(C=S)}$.

(**C9**)[Ni(dmit)$_2$]; Anal. Found: C, 33.89; H, 4.26; N, 2.51%. Calcd for $C_{18}H_{28}NS_{10}Ni$: C, 33.90; H, 4.43; N, 2.20%. IR (KBr): 1340 cm^{-1} for $\nu_{(C=C)}$, 1060 cm^{-1} for $\nu_{(C=S)}$.

(**C10**)[Ni(dmit)$_2$]; Anal. Found: C, 35.12; H, 4.53; N, 2.16%. Calcd for $C_{19}H_{30}NS_{10}Ni$: C, 35.01; H, 4.64; N, 2.15%. IR (KBr): 1342 cm^{-1} for $\nu_{(C=C)}$, 1060 cm^{-1} for $\nu_{(C=S)}$.

(**C11**)[Ni(dmit)$_2$]; Anal. Found: C, 35.97; H, 4.74; N, 2.35%. Calcd for $C_{20}H_{32}NS_{10}Ni$: C, 36.08; H, 4.84; N, 2.10%. IR (KBr): 1341 cm^{-1} for $\nu_{(C=C)}$, 1061 cm^{-1} for $\nu_{(C=S)}$.

(**C12**)[Ni(dmit)$_2$]; Anal. Found: C, 37.34; H, 4.73; N, 2.02%. Calcd for $C_{21}H_{34}NS_{10}Ni$: C, 37.10; H, 5.04; N, 2.06%. IR (KBr): 1345 cm^{-1} for $\nu_{(C=C)}$, 1061 cm^{-1} for $\nu_{(C=S)}$.

(**C13**)[Ni(dmit)$_2$]; Anal. Found: C, 37.89; H, 4.94; N, 2.04%. Calcd for $C_{22}H_{36}NS_{10}Ni$: C, 38.08; H, 5.23; N, 2.02%. IR (KBr): 1344 cm^{-1} for $\nu_{(C=C)}$, 1062 cm^{-1} for $\nu_{(C=S)}$.

(**C14**)[Ni(dmit)$_2$]; Anal. Found: C, 39.10; H, 5.25; N, 2.01%. Calcd for $C_{23}H_{38}NS_{10}Ni$: C, 39.02; H, 5.41; N, 1.98%. IR (KBr): 1340 cm^{-1} for $\nu_{(C=C)}$, 1060 cm^{-1} for $\nu_{(C=S)}$.

(**C15**)[Ni(dmit)$_2$]; Anal. Found: C, 39.68; H, 5.36; N, 1.97%. Calcd for $C_{24}H_{40}NS_{10}Ni$: C, 39.93; H, 5.58; N, 1.94%. IR (KBr): 1346 cm^{-1} for $\nu_{(C=C)}$, 1055 cm^{-1} for $\nu_{(C=S)}$.

(**C16**)[Ni(dmit)$_2$]; Anal. Found: C, 40.84; H, 5.55; N, 1.96%. Calcd for $C_{25}H_{42}NS_{10}Ni$: C, 40.80; H, 5.75; N, 1.90%. IR (KBr): 1345 cm^{-1} for $\nu_{(C=C)}$, 1059 cm^{-1} for $\nu_{(C=S)}$.

(**C17**)[Ni(dmit)$_2$]; Anal. Found: C, 41.61; H, 5.72; N, 1.90%. Calcd for $C_{26}H_{44}NS_{10}Ni$: C, 41.64; H, 5.91; N, 1.87%. IR (KBr): 1344 cm^{-1} for $\nu_{(C=C)}$, 1059 cm^{-1} for $\nu_{(C=S)}$.

(**C18**)[Ni(dmit)$_2$]; Anal. Found: C, 42.43; H, 5.98; N, 1.89%. Calcd for $C_{27}H_{46}NS_{10}Ni$: C, 42.45; H, 6.07; N, 1.83%. IR (KBr): 1347 cm^{-1} for $\nu_{(C=C)}$, 1059 cm^{-1} for $\nu_{(C=S)}$.

Measurements. IR spectra (KBr pellets) were measured using a JASCO FT/IR-410 spectrophotometer, with a resolution of 4 cm^{-1}. Elemental analysis data were obtained with a Perkin-Elmer 2400II CHN analyzer.

X-ray Crystallography. A single crystal was mounted on a glass capillary. Intensity data were collected at 173 K with a Bruker AXS SMART diffractometer equipped with a CCD area detector and Mo Kα ($\lambda = 0.71073$ Å) radiation. The structures were solved and refined with SHELX-97[33] using the direct method and expanded using Fourier techniques. All non-hydrogen atoms were refined anisotropically by the full-matrix least-square method. Some hydrogen atoms were found from experimental data directly, and their position and isotropic thermal parameters were refined. Selected crystallographic data are summarized in Table 1. Crystallographic data have been deposited at the Cambridge Crystallographic Data Centre: Deposit numbers CCDC-796601–796610 and 796612–796616 for compounds **C*n*** ($n = 3$ and 5–18) complex salts, respectively. Copies of the data can be obtained free of charge via http://www.ccdc.cam.ac.uk/conts/retrieving.html (or from the Cambridge Crystallographic Data Centre, 12, Union Road, Cambridge, CB2 1EZ, U.K.; FAX: +44 1223 336033; e-mail: deposit@ccdc.cam.ac.uk).

Results and Discussion

Fifteen single crystals of alkyltrimethylammonium–[Ni(dmit)$_2$] salts were obtained from acetone and methanol solutions. The crystal data are shown in Table 1. Measured temperatures of X-ray crystallographic analysis were 173 K, except for **C17** complex salt (297 K).

Crystal Structures of the Complex Salts. Table 1 shows that **C3** complex salt crystallized in monoclinic space group $C2/c$, while other complex salts adopted triclinic space group $P\bar{1}$. The number of molecules in a unit cell (Z) is essentially equal to 2 in **C5**–**C18** complex salts, but in **C8** complex salt, it is 4. In the case of **C8** complex salt, the asymmetric unit consists of two cation/anion pairs. Thus, the crystal of **C8** complex salt might be a different polymorph form from the others, but only single crystals with the observed lattice parameters could be obtained. The densities of crystals calculated from X-ray data tend to decrease with an increase of the carbon number. However, the density of **C12** complex salt, 1.512 mg cm^{-3}, is larger than those of **C11** and **C13** complex salts, 1.502 and 1.481 mg cm^{-3}, respectively. As will be described in more detail

Table 1. Crystal Data of Complex Salts

		Compound						
		(**C3**)[Ni(dmit)$_2$]	(**C5**)[Ni(dmit)$_2$]	(**C6**)[Ni(dmit)$_2$]	(**C7**)[Ni(dmit)$_2$]	(**C8**)[Ni(dmit)$_2$]	(**C9**)[Ni(dmit)$_2$]	(**C10**)[Ni(dmit)$_2$]
Formula		$C_{12}H_{16}NNiS_{10}$	$C_{14}H_{20}NNiS_{10}$	$C_{15}H_{22}NNiS_{10}$	$C_{16}H_{24}NNiS_{10}$	$C_{17}H_{26}NNiS_{10}$	$C_{18}H_{28}NNiS_{10}$	$C_{19}H_{30}NNiS_{10}$
Fw		553.57	581.62	595.65	609.67	623.70	637.72	651.75
T/K		173	173	173	173	173	173	173
Crystal system		Monoclinic	Triclinic	Triclinic	Triclinic	Triclinic	Triclinic	Triclinic
Space group		$C2/c$	$P\bar{1}$	$P\bar{1}$	$P\bar{1}$	$P\bar{1}$	$P\bar{1}$	$P\bar{1}$
Unit cell	a/Å	19.235(2)	8.0755(7)	8.2667(8)	8.1401(6)	13.720(4)	8.150(4)	8.1143(9)
	b/Å	17.615(2)	12.0608(11)	12.0965(12)	12.2681(10)	13.787(4)	12.772(6)	12.2084(13)
	c/Å	14.240(2)	12.7621(11)	12.7074(13)	13.0992(10)	15.842(4)	14.082(6)	15.8379(17)
	α/deg		80.153(2)	78.155(2)	76.3220(10)	66.707(3)	71.647(5)	69.290(2)
	β/deg	61.142(2)	76.702(10)	77.511(2)	73.5060(10)	79.470(4)	80.628(6)	75.866(2)
	γ/deg		81.257(2)	80.636(2)	89.1520(10)	69.680(3)	81.246(6)	78.928(2)
Volume/Å^3		4225.8(9)	1167.87(18)	1185.4(2)	1216.81(16)	2577.6(12)	1340.0(10)	1413.4(3)
Z		8	2	2	2	4	2	2
δ_{calcd}/Mg m^{-3}		1.740	1.654	1.669	1.664	1.607	1.581	1.531
GOF a)		0.868	0.896	0.878	0.814	0.837	0.913	1.081
Final R	$R1$ b)	0.03106	0.0275	0.0305	0.0279	0.0385	0.0567	0.0491
Indices [$I > 2\sigma(I)$]	$wR2$ c)	0.0600	0.0627	0.0720	0.0921	0.1076	0.1332	0.1096
R indices	$R1$ b)	0.0614	0.0383	0.0425	0.0316	0.0675	0.1580	0.0585
(all data)	$wR2$ c)	0.0661	0.0652	0.0752	0.0986	0.1364	0.1974	0.1148

Continued on next column.

Table 1. *Continued.*

		Compound							
		(**C11**)[Ni(dmit)$_2$]	(**C12**)[Ni(dmit)$_2$]	(**C13**)[Ni(dmit)$_2$]	(**C14**)[Ni(dmit)$_2$]	(**C15**)[Ni(dmit)$_2$]	(**C16**)[Ni(dmit)$_2$]	(**C17**)[Ni(dmit)$_2$]	(**C18**)[Ni(dmit)$_2$]
Formula		$C_{20}H_{32}NNiS_{10}$	$C_{21}H_{34}NNiS_{10}$	$C_{22}H_{36}NNiS_{10}$	$C_{23}H_{38}NNiS_{10}$	$C_{24}H_{40}NNiS_{10}$	$C_{25}H_{42}NNiS_{10}$	$C_{26}H_{44}NNiS_{10}$	$C_{27}H_{46}NNiS_{10}$
Fw		665.78	679.80	693.83	707.85	721.88	735.91	749.93	763.96
T/K		173	173	173	173	173	173	297	173
Crystal system		Triclinic	Triclinic	Triclinic	Triclinic	Triclinic	Triclinic	Triclinic	Triclinic
Space group		$P\bar{1}$	$P\bar{1}$	$P\bar{1}$	$P\bar{1}$	$P\bar{1}$	$P\bar{1}$	$P\bar{1}$	$P\bar{1}$
Unit cell	a/Å	9.6430(8)	9.569(2)	9.752(2)	8.0131(11)	9.744(2)	7.7999(15)	9.8139(8)	7.747(3)
	b/Å	10.0712(8)	10.061(2)	10.000(2)	12.2226(17)	10.003(2)	12.296(2)	10.1853(8)	12.320(5)
	c/Å	16.4924(14)	16.780(4)	16.923(3)	16.985(2)	17.929(4)	18.473(4)	19.5086(16)	19.877(7)
	α/deg	73.7090(10)	74.960(3)	79.468(3)	86.841(3)	84.721(4)	86.853(3)	87.385(2)	80.534(5)
	β/deg	88.9310(10)	88.565(3)	84.896(2)	79.046(3)	80.195(3)	79.371(3)	76.070(2)	80.819(4)
	γ/deg	73.7170(10)	73.382(3)	73.675(2)	78.755(2)	73.365(3)	78.733(3)	72.839(2)	78.468(5)
Volume/Å^3		1472.6(2)	1493.0(6)	1556.0(6)	1601.6(4)	1648.2(7)	1700.1(6)	1807.7(3)	1796.8(11)
Z		2	2	2	2	2	2	2	2
δ_{calcd}/Mg m^{-3}		1.502	1.512	1.481	1.468	1.455	1.438	1.378	1.412
GOF a)		0.665	0.758	1.074	0.0739	0.799	0.868	0.818	0.829
Final R	$R1$ b)	0.0266	0.0329	0.0483	0.0470	0.0449	0.0372	0.0445	0.0412
Indices [$I > 2\sigma(I)$]	$wR2$ c)	0.0810	0.0945	0.1569	0.0886	0.1145	0.1049	0.0948	0.1087
R indices	$R1$ b)	0.0315	0.0400	0.0603	0.1259	0.0956	0.0549	0.0984	0.0751
(all data)	$wR2$ c)	0.0898	0.1046	0.1716	0.1363	0.1508	0.1280	0.1222	0.1414

a) Goodness-of fit on F^2. b) $R_1 = \sum||F_o| - |F_c||/\sum|F_o|$. c) $wR2 = \sum[w(F_o^2 - F_c^2)^2]/\sum[w(F_o^2)^2]]^{1/2}$.

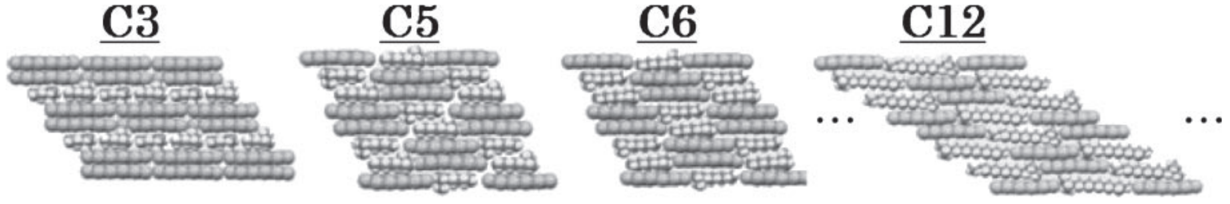

Figure 1. Crystal packing structures of (**C3**)[Ni(dmit)$_2$], (**C5**)[Ni(dmit)$_2$], (**C6**)[Ni(dmit)$_2$], and (**C12**)[Ni(dmit)$_2$]. Cations and anions are distinguished by white and gray, respectively.

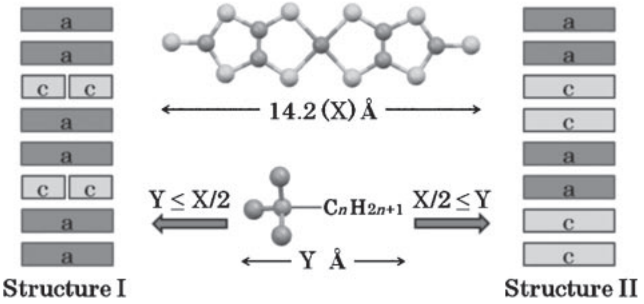

Figure 2. Schematic diagram of stacking structures **I** and **II**. Characters a and c represent anion and cation, respectively.

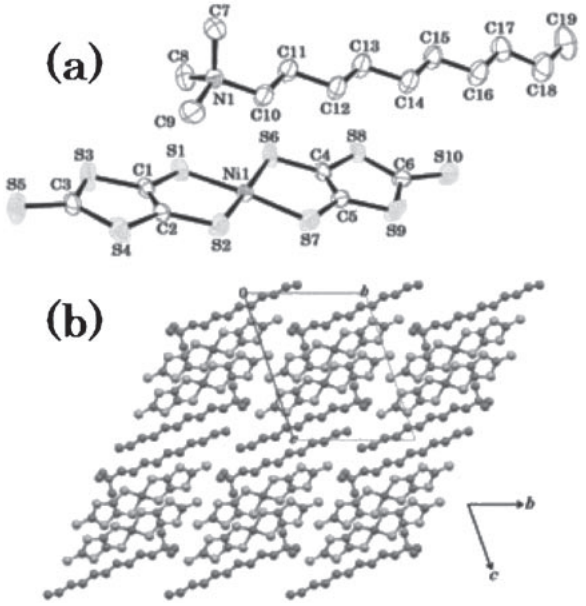

Figure 3. ORTEP III view of (a) an ion pair with numbering scheme and (b) crystal structure of (**C10**)[Ni(dmit)$_2$]. Hydrogen atoms are omitted for clarity. Displacement ellipsoids are drawn at the 50% probability level, hereafter.

later in the text, the crystal packing of **C12** complex salt became denser because of the end-*gauche* conformation of the dodecyl group present only in this complex salt.

The crystal packing structures in Figure 1 show that the layers of [Ni(dmit)$_2$]$^-$ anions and the layers of cations are alternately piled up, and the anions formed dimers by stacking. This structural characteristic is commonly observed in all crystals. However, stacking structure clearly differed between **C3** and other complex salts. Adjacent cations were aligned along the long axis of [Ni(dmit)$_2$]$^-$ anion in **C3** complex salt, while those of other salts were aligned toward the short axis of [Ni(dmit)$_2$]$^-$ anion. The lengths of cations were 4.8828(42) (C9···C12 distance), 7.4615(39) (C9···C14 distance), 8.7631(44) (C9···C15 distance), and 14.5729(40) Å (C8···C21 distance) for **C3**, **C5**, **C6**, and **C12** complex salts, respectively, and the length of anion was about 14.2 Å (S5–S10 distance) for all complex salts. These data indicate that the length of cation in **C3** complex salt is shorter than half the length of [Ni(dmit)$_2$]$^-$ anion, while that of other complex salt with longer alkyl chain is longer. This difference led to the difference in crystal structure as schematically shown in Figure 2. Thus the crystal structures can be classified into two categories, structures **I** and **II**. **C3** complex salt adopted structure **I**, because the length of the cation is shorter than half the length of [Ni(dmit)$_2$]$^-$ anion. By adopting this structure **I**, cations can attain closer contact with the anions. These results indicate that different stacking structures arose from "correlativity in the lengths of long axis of cation and anion" principle, namely CLCA. It is well-known that the matching of the sizes of counter ions is important in the crystallization process.[34,35] CLCA can be regarded as a special case of this principle for the salts of ions with relatively elongated molecular shape. The feature of CLCA principle will be discussed later in the text.

Commonly observed structural characteristics of complex salts are described below using the crystal structure of **C10** complex salt shown in Figure 3 as an example. ORTEP plot of an ion pair shown in Figure 3a with the atomic numbering scheme exhibits a close contact of N$^+$ in ammonium cation and thiolate S$^-$ in the dmit moiety of the anion. This suggests the presence of strong electrostatic interaction in the crystal. Alkyl chain nestles along the anion in the direction of long molecular axis of [Ni(dmit)$_2$]$^-$ anion. On the other hand, the crystal packing in Figure 3b shows that two anions face each other to form a dimer by π–π interaction, and two cations are in contact with each other to form a dimer by hydrophobic interaction between the alkyl groups.

In addition, structural characteristics of **C5–C10** complex salts are found to be fundamentally similar, while structural characteristics in **C*n*** complex salts with *n* exceeding 10 exhibit notable differences between odd- and even-numbered **C*n*** complex salts. It is generally accepted that the hydrophobic interaction between long alkyl chains becomes enhanced by elongation of the chain length *n*, and it often predominates other intermolecular interactions when *n* exceeds ca. 10. This effect leads to the characteristic nature of the compound with long alkyl groups, such as surfactants, lipids, greasy oils, etc. Thus, the observed difference between short and long alkyl substituted analogs can be attributed to this effect.

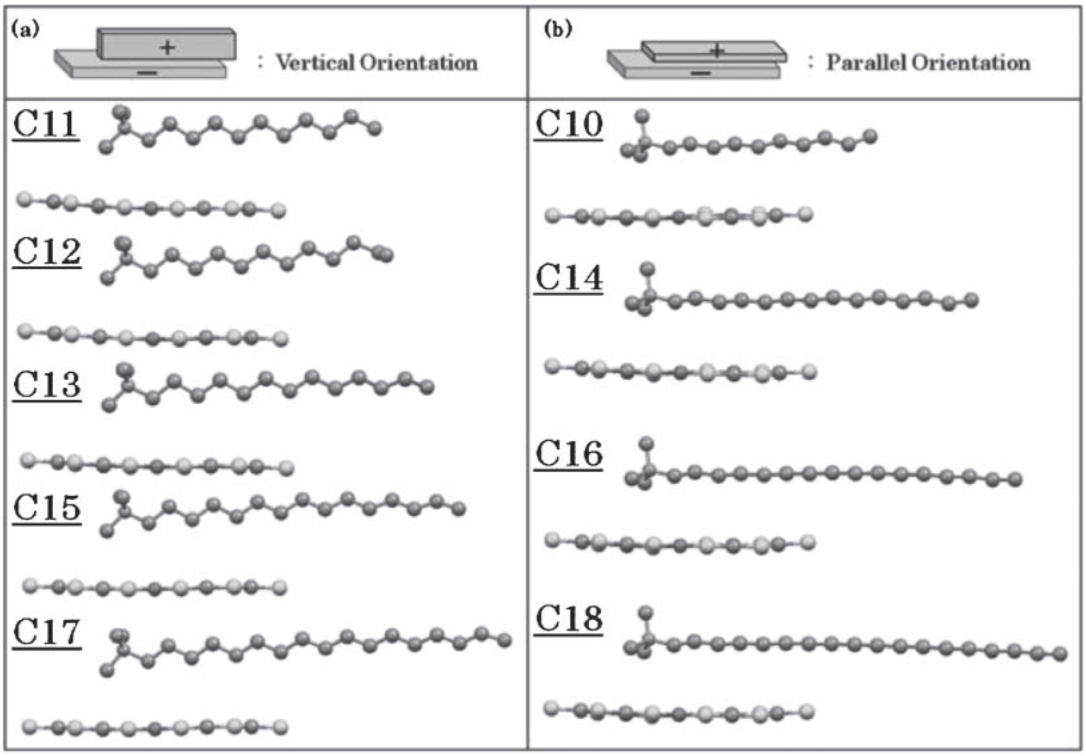

Figure 4. Two types of orientation for alkyl chain; (a) vertical and (b) parallel orientations relative to the molecular plane of anion.

Odd–Even Effect in the Crystal Structure of C10–C18 Complex Salts. When the structures of ion pairs in crystals are thoroughly investigated, we found an interesting odd–even effect in their structures. It is well known that the alkyl chains tend to adopt the most stable all-*trans* conformation. In all the crystals investigated, alkyl chains adopted all-*trans* conformation with the exception of **C12** complex salt in which the end methyl group of dodecyl chain adopted *gauche* conformation, i.e., the end-*gauche* conformation. We concluded that the crystal structure of **C12** complex salt is exceptional, thus we decided to discuss separately later in the text. As can be seen in Figure 3, the plane of decyl chain extends parallel to the plane of [Ni(dmit)$_2$]$^-$ anion. Note that the C7 methyl group sticks out normal to the plane of [Ni(dmit)$_2$]$^-$ anion. However, in **C11**–**C13**, **C15**, and **C17** complex salts, the direction is inverted as shown in Figure 4. With the exception of **C12** complex salt, the crystal structure exhibited a clear odd–even effect.

In order to elucidate the structural difference between two crystal packing structures, structural parameters were thoroughly investigated. In the cations, all alkyl chains except for **C12** complex salt adopted all-*trans* conformation with dihedral angles, C–C bond lengths and C–C–C bond angles of the alkyl chains being within the region of 171.5(5)–179.9(3)°, 1.469(7)–1.529(5) Å and 109.0(3)–119.6(7)°, respectively. These data are in close agreement with the values previously reported for long alkyl chains of related compounds.[36,37] In [Ni(dmit)$_2$]$^-$ anions, the bond length of C=C of dmit moieties are 1.347(7)–1.363(2) Å, indicating that the complex is monovalent.[38] Coordination geometries of [Ni(dmit)$_2$] were essentially square-planar, and the Ni–S distances were 2.1471(16)–2.1654(6) Å, and *cis*-S–Ni–S angles were 86.67(2)–93.30(2)°, which are also normal values for the monovalent complex.

With regard to the intermolecular interactions, [Ni(dmit)$_2$]$^-$ anions in the case of even-numbered **C*n*** complex salts (excluding **C12**) are dimerized by a face-to-face stack with sulfur–sulfur contacts (3.5631(1)–3.679(2) Å) shorter than the sum of the van der Waals radii. The dimer is found to form further sulfur–sulfur contacts with adjacent dimers by side-by-side interaction (3.5962(17)–3.695(2) Å). In the case of odd-numbered **C*n*** complex salts, anions form dimers but with no sulfur–sulfur contact. However, sulfur–sulfur contacts of dimers by side-by-side interaction (3.4903(14)–3.694(2) Å) are also present, in this case. As noted previously, all complex salts are found to be composed of alternate layers of [Ni(dmit)$_2$]$^-$ anions and cations (Figure 3b). Ni–N$^+$ distances were 4.569(3)–4.624(3) and 4.716(3)–4.741(2) Å for even and odd numbered **C*n*** complex salts, respectively. Therefore, the distances in even-numbered **C*n*** complex salts with parallel orientation tend to be shorter than the distances in odd-numbered **C*n*** complex salts with vertical orientation. Ni–N$^+$ distances versus the number of carbon atoms in the alkyl chain for **C*n*** complex salts are given in Figure 5. As is evident in Figure 5, Ni–N$^+$ distances in the case of **C10**–**C18** complex salts also exhibit a clear odd–even effect.

Crystal data in Table 1 also exhibit odd–even effect. When the number of carbon atoms in alkyl chain is odd, the values of *a* axis tends to be longer while that of *b* axis shorter, and the angle α tends to be smaller than those in the case of even-numbered complex salts with the exception of **C12** complex salt. As previously pointed out, **C12** complex salt is exceptional and its lattice parameters are similar to those of odd-numbered complex salts.

Crystal packing along the *a* axis shown in Figure 6 for **C11** complex salt shows that the structure of **C11** complex salt with

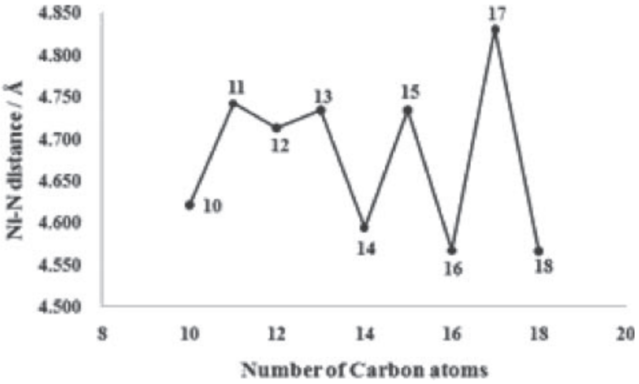

Figure 5. Dependence of Ni–N^+ distance on the number of carbon atoms.

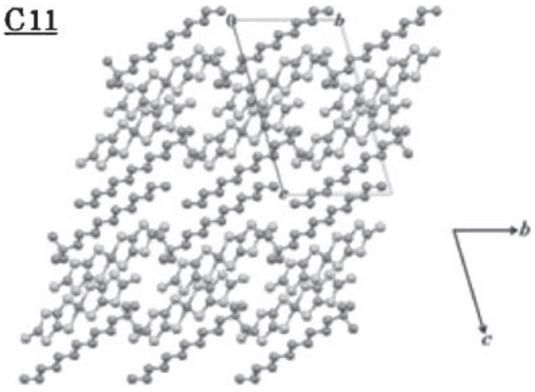

Figure 6. Molecular packing of (**C11**)[$Ni(dmit)_2$]. Hydrogen atoms are omitted for clarity.

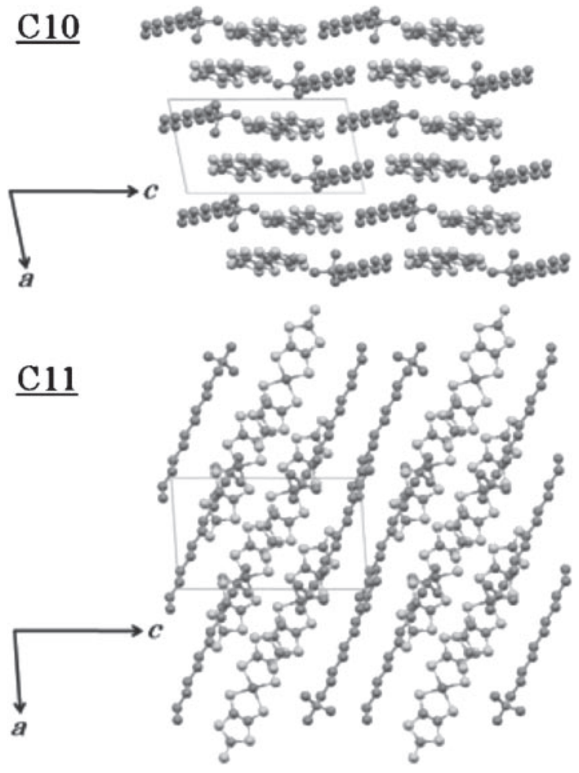

Figure 7. Molecular packings of (**C10**)[$Ni(dmit)_2$] and (**C11**)[$Ni(dmit)_2$] along *b* axis. Hydrogen atoms are omitted for clarity.

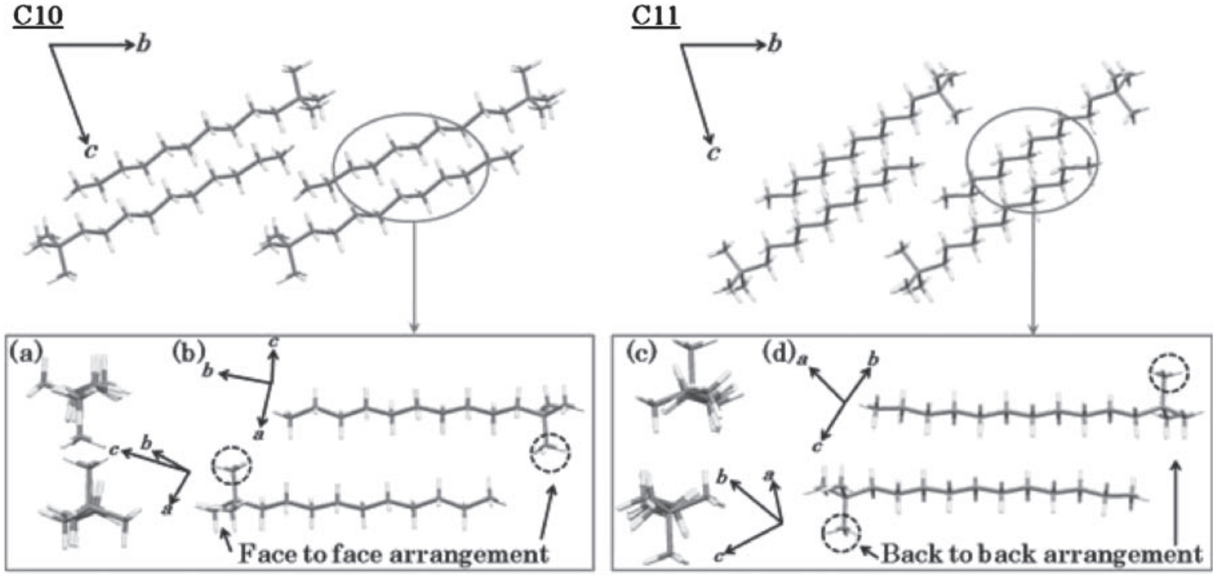

Figure 8. View along molecular axis (a, c) and side view (b, d) of neighboring cations for (**C10**)[$Ni(dmit)_2$] (a, b) and (**C11**)[$Ni(dmit)_2$] (c, d).

an odd-numbered alkyl chain is similar to the structure of **C10** complex salt with even-numbered alkyl chain given in Figure 3b as a whole. However, views along the *b* axis given in Figure 7 show clear difference between them. The values of *a* and *b* axes are 8.1143(9) and 12.2084(13) Å for **C10** complex salt, and 9.6430(8) and 10.0712(8) Å for **C11** complex salt, respectively. This difference reflects parallel or vertical orientation of ion pairs in Figure 4.

Relative arrangement of the nearest neighboring cations is given in Figure 8. View along molecular axis (a, c) and side view (b, d) clearly exhibit the difference between the structures of **C10** and **C11** complex salts. Two *N*-methyl groups (C7) of neighboring cations are facing each other in **C10** complex salt, while those in **C11** complex salt are oriented in opposite direction. When the carbon number of the alkyl chain is even (**C10**), the end-methyl group is located close to the β-carbon of the neighboring alkyl chain. Thus, *N*-methyl groups (C7) have enough space to adopt face-to-face arrangement, which leads to a closer packing. In contrast, when the carbon number is odd (**C11**), the end-methyl group is located close to the α-carbon of the neighboring alkyl chain. This structural feature, as a consequence, does not provide enough space for *N*-methyl group (C7) to adopt face-to-face arrangement. Accordingly, *N*-methyl group (C7) is distantly positioned from the end-methyl group to avoid steric hinderance between them. The difference in the arrangement of *N*-methyl groups resulted in the structural difference of ion pair (Figure 4).

Crystal Structure of C12 Complex Salt. Structure of **C12** complex salt has already been reported,[39] but its unusual aspect was not recognized at that time. Interestingly, our study revealed that the structural features of **C12** complex salt show different trend from those of other even-numbered complex salts. As previously discussed, alkyl chains of other complex salts adopt all-*trans* conformation, but the end methyl group of dodecyl chain of **C12** complex salt adopt *gauche* conformation. The torsion angle (C18–C19–C20–C21) of end methyl group is 70.4(3)°, while the other torsion angles are within the range of 174.7(2)–180.0(2)°. The formation of end-*gauche* conformation results in the shortening of the dodecyl chain length. It should be noted that the length (14.5729(40) Å) of **C12** cation shortened by the end-*gauche* conformation nearly fits the length (14.220(3) Å) of long axis of [Ni(dmit)$_2$]$^-$ anion. It is likely that such a coincidence in molecular length should be suitable for piling them alternately in the crystal packing. Thus we believe that the formation of end-gauche conformation is caused by the correlativity in the lengths of long axis of cation and anion (CLCA principle). The shortening of the length of dodecyl chain by end-*gauche* conformation causes **C12** cation to act as **C11** cation in crystal, and consequently changes the orientation of ion pair from usual parallel orientation for even-numbered cations to vertical orientation of odd-numbered cations. As a result, we obtained two examples of crystal systems involving CLCA principle.

Conclusion

We have prepared fifteen 1:1 complex salts composed of [Ni(dmit)$_2$]$^-$ anion and alkyltrimethylammonium (**C3** and **C5**–**C18**) cations to examine the structural change in crystalline state depending on the alkyl chain length. We have shown that the molecular arrangement arose from "correlativity in the lengths of long axis of cation and anion" principle, namely **CLCA**, and the orientation between the alkyl chain of cation and [Ni(dmit)$_2$]$^-$ anion differed between the odd- and even-numbered **C*n*** complex salts with *n* exceeding 10. Furthermore, **C12** shortened its molecular length by adopting unusual end-*gauche* conformation due to **CLCA** and the structural features of its complex salt differed from those of even-numbered **C*n*** complex salts, and became very similar to that of **C11** complex salt having odd-numbered alkyl chain.

Supporting Information

Data of geometric parameters, lengths of [Ni(dmit)]$^-$ anion and cation, Ni–N$^+$ distance in ion pair and distances/Å of sulfur–sulfur interactions. This material is available free of charge on the web at http://www.csj.jp/journals/bcsj/.

References

1 M. R. Andersson, Q. Pei, T. Hjertberg, O. Inganäs, O. Wennerström, J.-E. Österholm, *Synth. Met.* **1993**, *55*, 1227.

2 C. Goosen, T. J. Laing, J. du Plessis, T. C. Goosen, G. L. Flynn, *Pharm. Res.* **2002**, *19*, 13.

3 M. Imit, T. Yamamoto, P. Imin, *J. Zhejiang Univ., Sci., B* **2005**, *6*, 365.

4 K. A. Aamer, G. N. Tew, *Macromolecules* **2007**, *40*, 2737.

5 M. Iida, C. Baba, M. Inoue, H. Yoshida, E. Taguchi, H. Furusho, *Chem.—Eur. J.* **2008**, *14*, 5047.

6 C. Gandolfi, C. Moitzi, P. Schurtenberger, G. G. Morgan, M. Albrecht, *J. Am. Chem. Soc.* **2008**, *130*, 14434.

7 K. Kubota, T. Kato, C. Adachi, *Appl. Phys. Lett.* **2009**, *95*, 073303.

8 O. A. Blackburn, B. J. Coe, J. Fielden, M. Helliwell, J. J. W. McDouall, M. G. Hutchings, *Inorg. Chem.* **2010**, *49*, 9136.

9 V. R. Thalladi, R. Boese, H.-C. Weiss, *Angew. Chem., Int. Ed.* **2000**, *39*, 918.

10 Y.-J. Han, J. Aizenberg, *Angew. Chem., Int. Ed.* **2003**, *42*, 3668.

11 Y.-Y. Lua, W. Jonathan, J. Fillmore, M. R. Linford, *Appl. Surf. Sci.* **2004**, *231–232*, 323.

12 S. Umadevi, A. Jákli, B. K. Sadashiva, *Soft Matter* **2006**, *2*, 875.

13 N. Fujita, Y. Sakamoto, M. Shirakawa, M. Ojima, A. Fujii, M. Ozaki, S. Shinkai, *J. Am. Chem. Soc.* **2007**, *129*, 4134.

14 F. Tao, S. L. Bernasek, *Chem. Rev.* **2007**, *107*, 1408.

15 K. G. Nath, O. Ivasenko, J. M. MacLeod, J. A. Miwa, J. D. Wuest, A. Nanci, D. F. Perepichka, F. Rosei, *J. Phys. Chem. C* **2007**, *111*, 16996.

16 C. Hägele, E. Wuckert, S. Laschat, F. Giesselmann, *ChemPhysChem* **2009**, *10*, 1291.

17 E. Mochizuki, N. Yasui, Y. Kai, Y. Inaki, N. Tohnai, M. Miyata, *Bull. Chem. Soc. Jpn.* **2000**, *73*, 1035.

18 A. G. L. Olive, G. Raffy, H. Allouchi, J.-M. Léger, A. D. Guerzo, J.-P. Desvergne, *Langmuir* **2009**, *25*, 8606.

19 P. Cassoux, L. Valade, H. Kobayashi, A. Kobayashi, R. A. Clark, A. E. Underhill, *Coord. Chem. Rev.* **1991**, *110*, 115.

20 H. Tanaka, Y. Okano, H. Kobayashi, W. Suzuki, A. Kobayashi, *Science* **2001**, *291*, 285.

21 R. Kato, *Chem. Rev.* **2004**, *104*, 5319.

22 T. Nakamura, H. Tanaka, M. Matsumoto, H. Tachibana, E. Manda, Y. Kawabata, *Synth. Met.* **1988**, *27*, 601.

23 Y. F. Miura, M. Horikiri, S. Tajima, T. Wakaita, S.-H. Saito, M. Sugi, *Synth. Met.* **2003**, *133–134*, 663.

24 Y.-L. Wang, D. Xu, W.-T. Yu, X.-Q. Wang, G.-H. Zhang, *Acta Crystallogr., Sect. E* **2006**, *62*, m757.

25 K. Honda, M. Goto, M. Kurahashi, Y. Miura, T. Nakamura, M. Matsumoto, Y. Kawabata, *Anal. Sci.* **1990**, *6*, 927.

26 Y. F. Miura, M. Horikiri, K. Honda, M. Shiro, K. Sasaki, M. Sugi, *Jpn. J. Appl. Phys.* **2004**, *43*, 2628.

27 K. Tomono, K. Ogawa, Y. Sasaki, K. Miyamura, *Inorg. Chim. Acta* **2008**, *361*, 269.

28 K. Onozaki, K. Miyamura, *Bull. Chem. Soc. Jpn.* **2006**, *79*, 876.

29 Y. Soneta, K. Miyamura, *Bull. Chem. Soc. Jpn.* **2006**, *79*, 282.

30 T. Koori, K. Tomono, K. Miyamura, *Acta Crystallogr., Sect. E* **2006**, *62*, m256.

31 E. Tomiyama, K. Tomono, D. Hashizume, T. Wada, K. Miyamura, *Bull. Chem. Soc. Jpn.* **2009**, *82*, 352.

32 G. Steimecke, R. Kirmse, E. Hoyer, *Z. Chem.* **1975**, *15*, 28.

33 G. M. Sheldrick, *SHELXS-97 and SHELXL-97, Program for the Solution of Crystal Structures*, University of Göttingen, Germany, **1997**.

34 S. A. Hodorowicz, E. K. Hodorowicz, H. A. Eick, *J. Solid State Chem.* **1983**, *50*, 180.

35 D. Braga, F. Grepioni, P. Milne, E. Parisini, *J. Am. Chem. Soc.* **1993**, *115*, 5115.

36 M. R. Silva, A. M. Beja, J. A. Paixão, *Acta Crystallogr., Sect. E* **2003**, *59*, o1151.

37 A. R. Campanelli, L. Scaramuzza, *Acta Crystallogr., Sect. C* **1986**, *42*, 1380.

38 L. Valade, J.-P. Legros, M. Bousseau, P. Cassoux, M. Garbauskas, L. V. Interrante, *J. Chem. Soc., Dalton Trans.* **1985**, 783.

39 Y. Yamamoto, K. Miyamura, Y. Gohshi, *Mol. Cryst. Liq. Cryst.* **1996**, *285*, 137.